



MULTI-MATERIAL OPTIMAL DESIGN OF 3D TRANSMISSION TOWERS USING BLACK HOLE MECHANICS OPTIMIZATION: REAL-SIZE EXAMPLES

P. Salmanpour^{*†}, A. Deylami, and M. Z. Kabir

Department of Civil & Environmental Engineering, Amirkabir University of Technology, Tehran, Iran

ABSTRACT

The multi-material size optimization of transmission tower trusses is carried out in the present study. Three real-size examples are designed, and statically analyzed, and the Black Hole Mechanics Optimization (BHMO) algorithm, a recently developed metaheuristic optimizer methodology, is employed. The BHMO algorithm's innovative search strategy, which draws inspiration from black hole quantum physics, along with a robust mathematical kernel based on the covariance matrix between variables and their associated costs, efficiently converges to global optimum solutions. Besides, three alloys of steel are taken into account in these examples for discrete size variables, each of which is defined in the problem by a weighted coefficient in terms of the elemental weight. The results also indicate that using multiple materials or alloys in addition to diverse cross-sectional sizes leads to the lowest possible cost and the most efficient solution.

Keywords: Transmission Tower Truss, Black Hole Mechanics Optimization, Multi-Material Optimization, Meta-Heuristic Algorithms, Covariance Matrix, 3D Optimization.

Received: 10 November 2024; Accepted: 22 December 2024

1. INTRODUCTION

Transmission towers are indispensable in the industrial landscape, serving as the linchpin for efficient electricity distribution. These structures, often inconspicuous yet vital, facilitate the transfer of power from remote generation plants to urban centers. Their significance lies in

^{*}Corresponding author: Department of Civil & Environmental Engineering, Amirkabir University of Technology, Tehran, Iran

[†]E-mail address: p.salmanpour.k@aut.ac.ir (P. Salmanpour)

forming resilient power grids that withstand adverse weather, ensuring uninterrupted electricity flow. Interconnecting networks, transmission towers allow surplus power transfer between regions, optimizing resource utilization. However, their optimization is imperative. Efficiency improvements and reduced energy losses contribute to sustainability, while cost-effective designs and technological advancements enhance the economic viability of power distribution systems. Incorporating smart grid technologies and eco-friendly practices not only improves performance but also minimizes the environmental impact. In essence, the careful optimization of transmission towers is crucial for bolstering the reliability, sustainability, and cost-effectiveness of power distribution networks, thereby shaping the future of industry and society.

The construction of transmission towers, which serve to keep conductors and ground wires, is now regarded as among the most crucial aspects of electrical power line transferring and distribution. In addition to their vital role in community development, their masts are thought to account for 35–45% of the cost of constructing electricity transmission lines [1]. In today's increasingly competitive economic world, possessing an optimal design at the lowest possible cost while providing acceptable performance and satisfying constraints is an integral component of any design [2]. Steel lattice truss transmission towers are typically preferred among concrete, steel polygonal, wood, and hybrid ones with regard to their high strength-to-weight ratio [3]. Truss structures are a broad class encompassing a variety of structure types including bridges, towers, cranes, etc. They are idealized as being simple to analyze and designed to withstand strong axial loads used for a variety of applications. Design variables associated with truss optimization problems include size (choosing the most optimal cross-section), layout (figuring out the optimum geometry), and topology (deciding on the most suitable number of parts) [4].

Numerous gradient-based mathematical approaches have been developed over the past few decades with the aim of solving optimization problems, but not all of them have proven effective for every problem. For instance, gradient-based optimization frameworks need to calculate a great deal of functional gradients in addition to an appropriate starting point. Likewise, the implementation of these methodologies becomes difficult and unstable in optimization problems when the objective function is complicated or contains multiple local optima [5]. Thus, researchers proposed metaheuristic algorithms as an effective alternative to common optimization techniques. These algorithms were inspired by metaphors from physics, mathematical rules, or other natural phenomena, such as swarm intelligence and evolution. Metaheuristic algorithms with repetitive behavior are capable of seeking global or near-global optimal solutions that are appropriate for an engineering design in discontinuous, non-smooth, complex, and NP-complete problems [6]. Hence, metaheuristic algorithms are increasingly gaining popularity in structural optimization applications due to their efficiency, such as their independence from gradient information and adept handling of constraints, as well as their reliability on promising solutions and robust performance in a wide range of applications [7]; as well, numerous metaheuristic algorithms have been developed and examined by scholars due to the no free lunch theorem [6–17], which claims that all optimization problems are unable to be solved by a single metaheuristic algorithm [10].

Transmission tower optimization was carried out using such dynamic [18] and non-linear programming [19] before 2000 when gradient-based methodologies were common;

however, this area of study with the aim of weight minimization as a function of the overall cost has been extensively examined over recent years by employing metaheuristic algorithms; for the paradigm, the following algorithms (or modified or hybrid ones)—genetic [1,20–22], simulated annealing [3,23,24], particle swarm optimization [25,26], firefly [9,27], and marine predators [11]—have dealt with transmission tower optimization problems with different kinds of design variables. In the current research, the cross-sectional areas and the materials used in components served as the design variables in a discrete space to optimize the transmission tower real-size examples. The multi-material optimization problems have been the subject of numerous studies in this field of study [9,26,28–31].

Metaheuristic algorithms can be categorized according to their metaphors, as previously mentioned. Genetic algorithms [32], particle swarm optimization [33], ant colony optimization [34], etc. are well developed by taking inspiration from phenomena of nature and animal behaviors such as biological laws and evolution. The principles and characteristics of the covariance matrix are also taken into consideration when developing the CMA-ES [35] and ECM [8], Black Hole Mechanics Optimization (BHMO) [6], and Enriched firefly algorithm [9]. As well, imperialist competitive algorithms [36] and teaching-learning-based optimization [37] have emerged by taking into account social behavior. Physical-based algorithms, such as simulated annealing [38], tabu search [39], harmony search [40], BHMO [6], and others, are one of the categories that interest scholars. The recently developed BMHO algorithm, which has not been used in transmission tower optimization, is chosen as the optimizer algorithm in this study. This algorithm has demonstrated significant outcomes in several kinds of optimization matters [6].

In spite of the considerable attention devoted by researchers to the optimization of transmission towers, the impact of employing multilateral approaches in structural design has not yet been adequately explored. Consequently, this study aims to concurrently examine the influence of material composition and cross-sectional area as design variables within an optimization framework. This approach has been applied to real-size structures, providing a practical example for the industry. The investigation is intended to fill the existing gap in understanding and contribute to the enhancement of transmission tower design methodologies.

The rest of the current study is organized as follows after this introduction. Section 2 presents a definition of the transmission tower metaheuristic-based optimum design. A brief overview of the BHMO algorithm's concept and formulation in section 3. In section 4, three transmission tower is chosen as a numerical example, and the results are given. Concluding remarks are included in section 5.

2. PROBLEM DEFINITION

According to earlier relevant research and using their notation, this section provides an overview introduction to the elements of truss structures in the multi-material size optimization problem [9].

2.1. Structural Design

The comprehensive design criteria of the AISC 360-22 code have been incorporated into

the structural design of transmission truss towers. In the following, some assumptions are provided.

2.2. Load Cases

Each example affects a single load case that is applied to the top nodes in the direction of x with a 100 kN force. Loads are applied gradually under static loading circumstances.

2.3. Structural Analysis

The direct stiffness method of the finite element method is used to perform the analysis of the spatial transmission tower trusses. Meanwhile, the effects of material and geometrical nonlinearity are disregarded; as an outcome, the linear-statical analysis is applicable.

2.4. Design Criteria

The AISC 360-22 code conditions must be addressed during the design phase with the aim of regulating elemental compressive and tensile strength. Constraints on active degrees of freedom in terms of displacement are likewise checked to be restricted for each transmission tower truss.

2.5. Structural Optimal Design

In this subsection, the optimum design of the transmission tower trusses utilizing metaheuristic algorithms is formulated and the problem is defined. However, within this framework, as previously pointed out, a metaheuristic algorithm seeks a possible superior solution by updating its mechanisms for a defined problem in each iteration to find the optimal solution. The answer for an engineering design is appropriate, even though there is no guarantee that the global optimum will be obtained [2].

2.6. Objective Function

The metaheuristic optimizer algorithm, as already mentioned before, addresses the minimization of the total elemental material weight of the transmission tower truss as a function of the overall cost. Thus, the objective function of an optimization problem involving different sizes of cross-sections with multiple materials can be written as Eq. (1):

$$W(x_{Discrete}) = \sum_{i=1}^{NE} \rho_i A_i L_i C_i \quad (1)$$

where $W(x_{Discrete})$ denotes the overall weight of the transmission tower truss with NE element number, and ρ_i , A_i , L_i , and C_i are respectively the material density, cross-sectional areas, length, and material alloy cost of the i^{th} element. It should be pointed out, that the algorithm seeks in a continuous search space; thus, by using Eq. (2) the continuous design vector ($x_{Continuous}$) can be transformed into a discrete search space ($x_{Discrete}$) according to [25].

$$x_{Discrete} = \text{floor}(x_{Continuous}) \quad (2)$$

2.7. Design Variables

The given list of sections includes 200 hole-circular sections with areas ranging from 0.1 cm² to 20 cm², with intervals of 0.1 cm², and with three different types of steel alloys. Therefore, the algorithm chooses intelligently from the 600 sections to use the cross-sectional areas of the list as design variables to decide on the optimum weight. These design variables have been summarized in Table 1.

Table 1: The design variables corresponding with the considered problems

| Problem | Material | Cross-Section Area |
|----------------------|----------|--------------------|
| Transmission Tower 1 | ✓ | ✓ |
| Transmission Tower 2 | ✓ | ✓ |
| Transmission Tower 3 | ✓ | ✓ |

2.8. Constraints Handling

Due to its simple manner of use, the penalty function method has been extensively utilized in the field of structural optimization among the different approaches to handling constraints in an optimization problem [12]; As it turns out, the following describes how the constraints in this study, which are dictated by elemental stress and nodal displacement, got handled (Eq. 3):

$$\begin{aligned}
 \sigma_{\min} \leq \sigma_e \leq \sigma_{\max} & \quad e = 1, 2, \dots, NE \\
 \delta_{\min} \leq \delta_d \leq \delta_{\max} & \quad d = 1, 2, \dots, ND \\
 A_{\min} \leq A_e \leq A_{\max} & \quad e = 1, 2, K, NE
 \end{aligned} \tag{3}$$

where σ , δ , A , and ND represent the elemental stress, nodal displacement, elemental cross-sectional area, and number of active degrees of freedom, respectively, and also, indices e and d are noted respectively current element and node.

The total violation is applied to the overall weight of the transmission tower truss in Eq. (1) when the criteria in Eq. (3) are violated as Eq. (4):

$$P(x) = (1 + \alpha v)^\beta \times W(x) \tag{4}$$

where $P(x)$ represents the penalized weight of the structure which should be minimized and v is the total violation; it should be noted that α and β are penalty coefficients set experimentally.

3. BLACK HOLE MECHANICS OPTIMIZATION

The Schwarzschild and Kerr black hole mechanics drawback in 2020 served as the basis for Kaveh et al.'s development of the BHMO algorithm. The BHMO utilizes a potent Kernel-based mathematical technique to evaluate the covariance matrix between each variable and

its relative cost with the aim of figuring out the most optimal orientation of variables. This strategy allows variables to be rapidly redirected to prevent trapping in local optima. This algorithm proved beneficial in several domains, including structural optimal design [6] and other areas [16]. In this section, the BHMO methodology and its computational details are briefly discussed in accordance with the developer's paper [6] as follows (for more details, please see the referenced work):

Step 1: Initialization

The initial variable positions of the BHMO are generated in the search space randomly, like the other metaheuristic algorithms. However, the difference is that the BHMO can direct each variable based on its relative cost directly to the global optima by utilizing the covariance matrix properties. Each particle is considered as a star and defined in a 4D space-time dimension, with each star's mass being a relative cost function.

Step 2: Creation of the Kerr Black Hole

In order to determine their relative cost as output and to create the covariance matrix, the objective function one can be evaluated using the input of random initial positions. Each variable must be considered separately in 2D space at the moment in order to compute covariance. At last, the Kerr black hole position can be chosen when data is transformed around a center. It should also be remarked that this phase serves as a global search strategy.

Step 3: Creation of the Schwarzschild Black Hole

It is necessary for establishing a local search mechanism since the Kerr black hole functions as a global search mechanism. Another benefit is that as the optimal solution is likely to be determined with the least amount of data after transformation, the neighborhood might be considered a key location when seeking the answer. As a result, it qualifies as the Schwarzschild black hole.

Step 4: Data Elimination

After re-evaluating and sorting the data in each phase, the distant data should be eliminated based on elite selection since the generation of data in each step will lead to a decrease in the algorithm's speed and efficiency.

Step 5: Termination Criteria

The procedure's termination criteria should be checked at the final stage of the entire procedure. In this work, a predetermined number of function evaluations (NFE) is set up for terminating the procedure when the constraints are not violated by the solution obtained by Eq. (4).

The flowchart of the computational details of the utilized method through this paper is illustrated in Fig. (1).

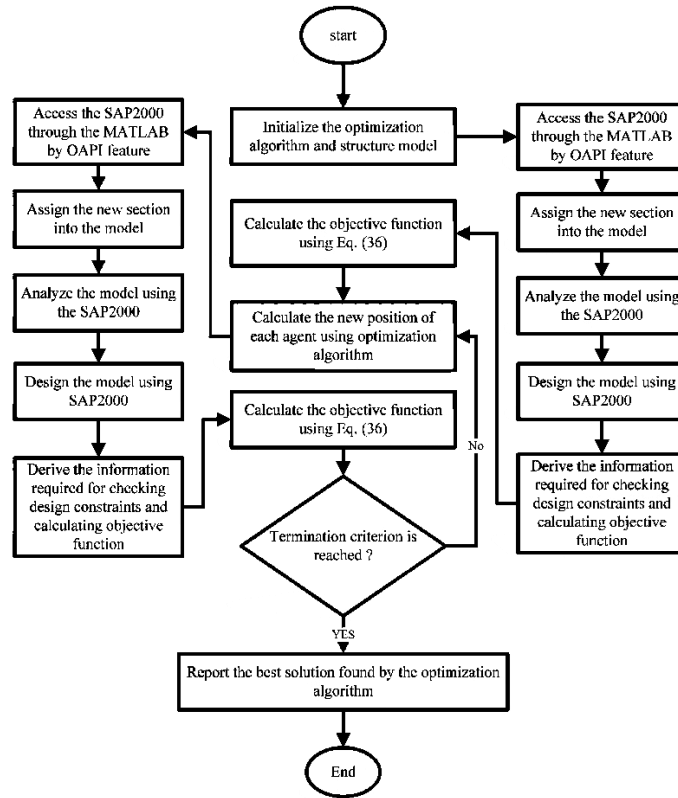


Figure 1: The computational details of the utilized method through the current paper

4. NUMERICAL EXAMPLES

This section features three real-size transmission tower truss examples for examination. The best possible outcome is chosen from 10 independent optimization procedures utilizing an Intel® Core™ i7 3600u CPU. To model, analyze, and design examples in accordance with AISC 360-22, the SAP2000 has been employed. Following that, the optimization framework is implemented in MATLAB® using the BHMO algorithm. As previously noted, the properties of the three types of steel material's alloy examined in this multi-material size optimization in 200 distinct size sections are tabulated in Table 2; The group design (variables) for each example should be noted as being equal to the number of elements and also to the material effects as an elemental cost coefficient, as shown in Eq. (1) by C_i .

Table 2: The utilized steel alloys through the current study.

| No. | Alloy | Elasticity Modulus (GPa) | Density (Kg/m ³) | Yield Stress | | Cost (Coefficient) |
|-----|-------|--------------------------|------------------------------|--------------|-------|--------------------|
| | | | | (MPa) | (ksi) | |
| 1 | S350 | 210 | 2768 | 350 | 52 | 0.35 |
| 2 | S500 | 210 | 2768 | 500 | 73 | 0.50 |
| 3 | S700 | 210 | 2768 | 700 | 102 | 0.70 |

4.1. Transmission Tower 1

In Fig. (2), the configuration of the first real-size example of transmission tower trusses is depicted which has 72 nodes and 132 element bars.

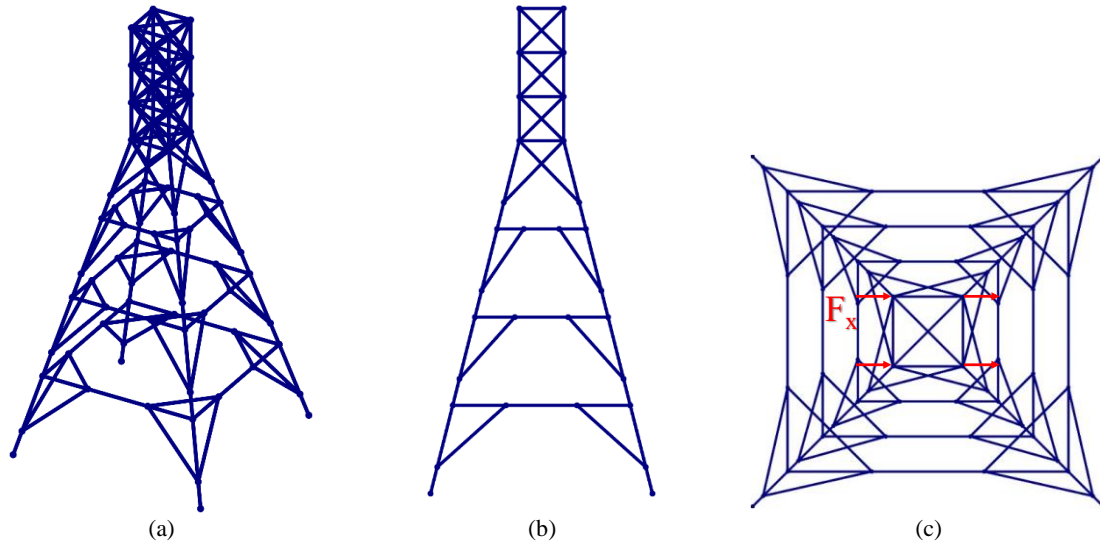


Figure 2: The initial configuration of the transmission tower 1: (a) 3D, (b) Front, and (c) Top views

Also, the nodal coordinates and the elemental connectivity of the example 1 tower structures are available in Complementary Tables (Tables C1 and C2).

The history of costs for each independent run is tabulated in Table 3, and Fig. (3) shows the convergence of the best one among the 10 independent runs and Table 4 dedicated how the BHMO algorithm solved the problem. Furthermore, Fig. (4) and (5) shown that the solution obtained without violation in terms of elemental stress and nodal displacement, and finally, Fig. (6) illustrates the schematic of the optimal design of the first example.

Table 3: The optimal cost of the structure achieved by BHMO through each independent optimization procedure (Example 1)

| NFE (%) | Run 1 | Run 2 | Run 3 | Run 4 | Run 5 | Run 6 | Run 7 | Run 8 | Run 9 | Run 10 |
|---------|--------|--------|--------|--------|--------|---------|---------|--------|---------|---------|
| 3 | 225.59 | 347.10 | 132.85 | 529.25 | 409.56 | 1219.34 | 1178.70 | 631.28 | 1293.48 | 1252.72 |
| 6 | 72.56 | 112.10 | 90.23 | 100.16 | 75.48 | 115.77 | 459.87 | 43.59 | 195.03 | 104.50 |
| 9 | 50.68 | 91.98 | 60.66 | 100.16 | 59.11 | 99.12 | 65.41 | 14.12 | 78.83 | 89.19 |
| 12 | 31.77 | 91.98 | 36.21 | 84.87 | 16.77 | 19.47 | 37.69 | 8.47 | 36.02 | 52.89 |
| 15 | 31.77 | 90.26 | 36.21 | 51.24 | 7.79 | 18.26 | 29.69 | 8.47 | 24.39 | 49.12 |
| 18 | 31.77 | 53.24 | 35.38 | 7.63 | 7.79 | 12.87 | 28.65 | 8.02 | 10.03 | 39.79 |
| 21 | 31.77 | 51.19 | 16.68 | 7.63 | 7.79 | 10.66 | 11.81 | 7.97 | 9.65 | 39.79 |
| 24 | 31.77 | 45.67 | 12.13 | 7.63 | 7.79 | 8.40 | 11.81 | 7.76 | 8.03 | 38.89 |
| 27 | 31.77 | 43.90 | 11.49 | 7.63 | 7.79 | 8.27 | 9.46 | 7.69 | 7.99 | 38.89 |
| 30 | 24.97 | 43.90 | 11.49 | 7.63 | 7.79 | 8.27 | 7.32 | 7.69 | 7.99 | 38.89 |
| 33 | 24.97 | 43.90 | 11.49 | 7.63 | 7.40 | 8.24 | 7.32 | 7.69 | 7.99 | 35.52 |
| 36 | 24.97 | 43.90 | 9.12 | 7.63 | 7.40 | 8.19 | 7.32 | 7.68 | 7.99 | 35.52 |
| 39 | 24.97 | 28.87 | 9.12 | 7.63 | 7.40 | 8.17 | 7.30 | 7.68 | 7.99 | 35.52 |
| 42 | 24.97 | 27.21 | 9.12 | 7.63 | 7.37 | 8.16 | 7.30 | 7.68 | 7.99 | 35.52 |
| 45 | 24.97 | 27.21 | 9.12 | 7.63 | 7.37 | 8.08 | 7.27 | 7.68 | 7.99 | 35.52 |

| | | | | | | | | | | |
|-----|-------|-------|------|------|------|------|------|------|------|-------|
| 48 | 24.97 | 27.21 | 9.12 | 7.63 | 7.35 | 8.00 | 7.27 | 7.68 | 7.99 | 35.09 |
| 51 | 24.97 | 26.79 | 9.12 | 7.63 | 7.31 | 8.00 | 7.27 | 7.67 | 7.99 | 32.35 |
| 54 | 24.97 | 15.24 | 9.12 | 7.62 | 7.30 | 8.00 | 7.27 | 7.67 | 7.99 | 30.22 |
| 57 | 24.97 | 15.24 | 9.12 | 7.62 | 7.30 | 7.99 | 7.27 | 7.66 | 7.99 | 30.22 |
| 60 | 24.97 | 15.24 | 8.37 | 7.62 | 7.30 | 7.99 | 7.27 | 7.64 | 7.99 | 27.95 |
| 63 | 24.97 | 15.24 | 8.37 | 7.56 | 7.30 | 7.99 | 7.27 | 7.64 | 7.99 | 27.95 |
| 66 | 24.97 | 15.24 | 8.37 | 7.56 | 7.30 | 7.99 | 7.27 | 7.64 | 7.96 | 27.95 |
| 70 | 24.97 | 15.24 | 8.37 | 7.54 | 7.30 | 7.99 | 7.27 | 7.64 | 7.94 | 27.95 |
| 75 | 24.97 | 15.24 | 8.37 | 7.54 | 7.26 | 7.99 | 7.27 | 7.64 | 7.91 | 27.95 |
| 80 | 24.97 | 15.24 | 7.96 | 7.54 | 7.26 | 7.98 | 7.27 | 7.64 | 7.91 | 27.95 |
| 85 | 24.97 | 15.24 | 7.96 | 7.54 | 7.26 | 7.98 | 7.27 | 7.64 | 7.91 | 27.95 |
| 90 | 24.97 | 15.24 | 7.96 | 7.53 | 7.26 | 7.98 | 7.27 | 7.64 | 7.91 | 27.95 |
| 95 | 24.97 | 15.24 | 7.96 | 7.51 | 7.26 | 7.98 | 7.27 | 7.64 | 7.91 | 27.95 |
| 98 | 24.97 | 15.24 | 7.96 | 7.47 | 7.25 | 7.98 | 7.27 | 7.64 | 7.90 | 27.95 |
| 100 | 24.97 | 15.24 | 7.96 | 7.47 | 7.25 | 7.98 | 7.27 | 7.64 | 7.90 | 27.95 |

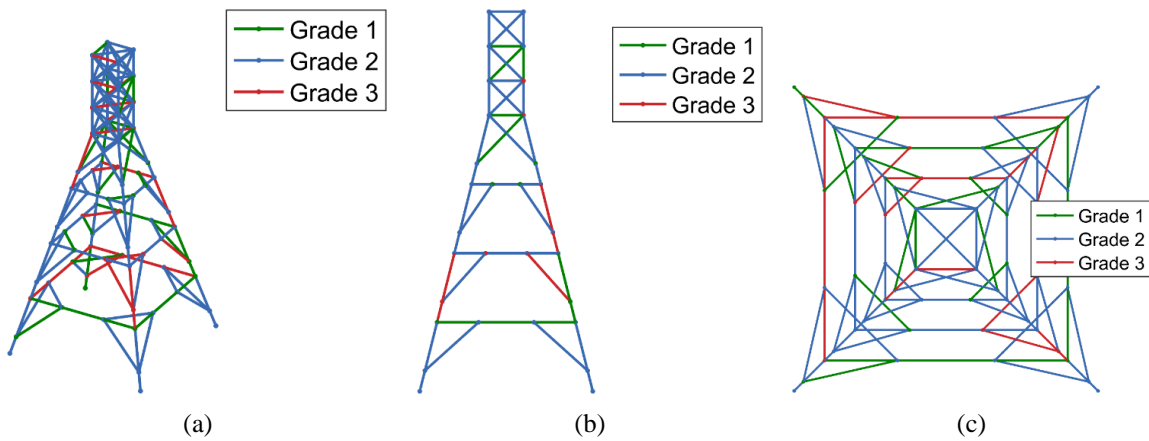


Figure 3: The optimized configuration of the transmission tower 1: (a) 3D, (b) Front, and (c) Top views

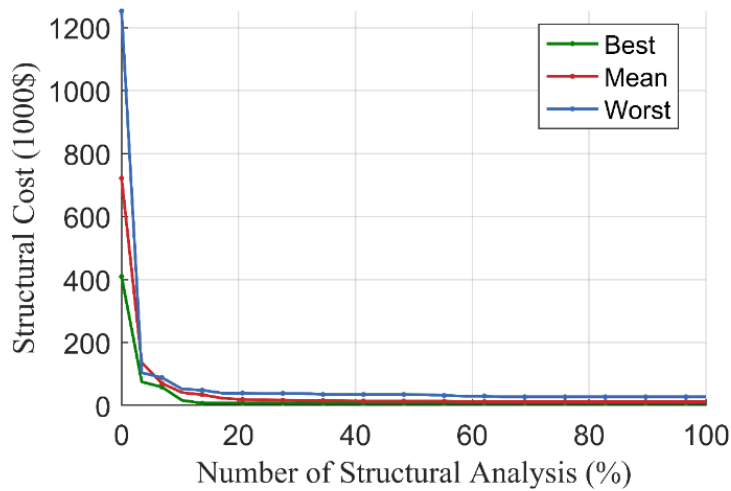


Figure 4: The optimization procedure of the transmission tower 1

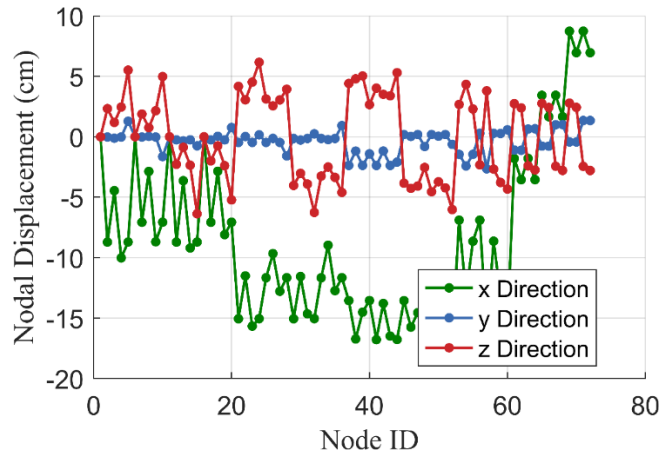


Figure 5: The nodal displacement of the transmission tower

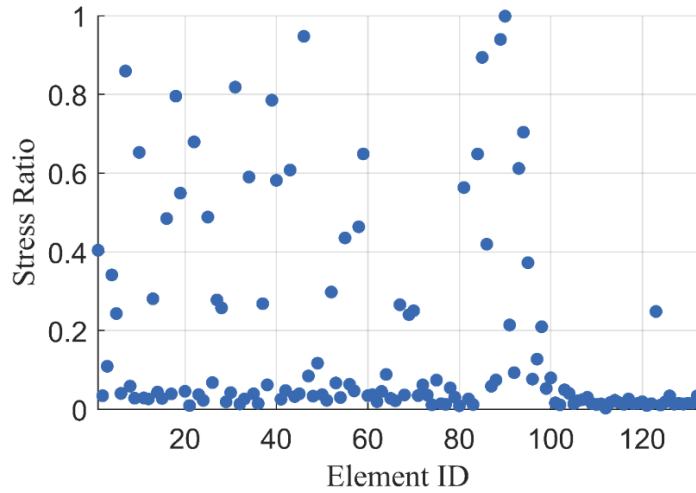


Figure 6: The element stress ratio of the transmission tower 1

Table 4: The optimal decision variables of the best solution (Example 1)

| Element ID | Radius (cm) | Area (cm ²) | Material | Element ID | Radius (cm) | Area (cm ²) | Material | Element ID | Radius (cm) | Area (cm ²) | Material |
|------------|-------------|-------------------------|----------|------------|-------------|-------------------------|----------|------------|-------------|-------------------------|----------|
| 1 | 9.70 | 295.59 | Grade_2 | 45 | 9.80 | 301.72 | Grade_2 | 89 | 7.60 | 181.46 | Grade_2 |
| 2 | 9.10 | 260.16 | Grade_2 | 46 | 10.60 | 352.99 | Grade_2 | 90 | 9.00 | 254.47 | Grade_1 |
| 3 | 9.50 | 283.53 | Grade_1 | 47 | 8.40 | 221.67 | Grade_2 | 91 | 8.50 | 226.98 | Grade_2 |
| 4 | 11.90 | 444.88 | Grade_1 | 48 | 8.20 | 211.24 | Grade_1 | 92 | 12.40 | 483.05 | Grade_2 |
| 5 | 4.90 | 75.43 | Grade_2 | 49 | 10.40 | 339.79 | Grade_2 | 93 | 11.90 | 444.88 | Grade_2 |
| 6 | 12.30 | 475.29 | Grade_3 | 50 | 10.30 | 333.29 | Grade_2 | 94 | 4.00 | 50.27 | Grade_3 |
| 7 | 10.50 | 346.36 | Grade_2 | 51 | 12.80 | 514.72 | Grade_2 | 95 | 7.30 | 167.42 | Grade_2 |
| 8 | 7.40 | 172.03 | Grade_2 | 52 | 8.40 | 221.67 | Grade_2 | 96 | 15.20 | 725.83 | Grade_2 |
| 9 | 9.30 | 271.72 | Grade_2 | 53 | 6.70 | 141.03 | Grade_2 | 97 | 9.70 | 295.59 | Grade_2 |
| 10 | 11.70 | 430.05 | Grade_2 | 54 | 7.50 | 176.71 | Grade_3 | 98 | 11.60 | 422.73 | Grade_1 |
| 11 | 10.20 | 326.85 | Grade_2 | 55 | 9.40 | 277.59 | Grade_2 | 99 | 8.80 | 243.28 | Grade_2 |
| 12 | 9.70 | 295.59 | Grade_2 | 56 | 12.60 | 498.76 | Grade_2 | 100 | 8.60 | 232.35 | Grade_1 |
| 13 | 10.10 | 320.47 | Grade_2 | 57 | 13.60 | 581.07 | Grade_2 | 101 | 9.60 | 289.53 | Grade_2 |
| 14 | 7.80 | 191.13 | Grade_2 | 58 | 8.70 | 237.79 | Grade_2 | 102 | 9.70 | 295.59 | Grade_2 |
| 15 | 13.80 | 598.28 | Grade_2 | 59 | 7.80 | 191.13 | Grade_2 | 103 | 10.80 | 366.44 | Grade_2 |

| Element ID | Radius (cm) | Area (cm ²) | Material | Element ID | Radius (cm) | Area (cm ²) | Material | Element ID | Radius (cm) | Area (cm ²) | Material | | | | |
|--------------------------------|-------------|-------------------------|----------|----------------|-------------|-------------------------|----------|-------------------------------|-------------|-------------------------|----------|---------------|--|--|--|
| 16 | 9.10 | 260.16 | Grade_2 | 60 | 14.60 | 669.66 | Grade_2 | 104 | 10.00 | 314.16 | Grade_2 | | | | |
| 17 | 5.60 | 98.52 | Grade_1 | 61 | 15.10 | 716.31 | Grade_2 | 105 | 12.70 | 506.71 | Grade_3 | | | | |
| 18 | 6.30 | 124.69 | Grade_2 | 62 | 7.60 | 181.46 | Grade_2 | 106 | 11.90 | 444.88 | Grade_2 | | | | |
| 19 | 11.70 | 430.05 | Grade_3 | 63 | 6.60 | 136.85 | Grade_2 | 107 | 10.00 | 314.16 | Grade_2 | | | | |
| 20 | 6.20 | 120.76 | Grade_2 | 64 | 10.60 | 352.99 | Grade_1 | 108 | 8.70 | 237.79 | Grade_1 | | | | |
| 21 | 14.70 | 678.87 | Grade_3 | 65 | 5.90 | 109.36 | Grade_2 | 109 | 7.20 | 162.86 | Grade_3 | | | | |
| 22 | 12.30 | 475.29 | Grade_1 | 66 | 10.50 | 346.36 | Grade_3 | 110 | 17.10 | 918.63 | Grade_2 | | | | |
| 23 | 8.20 | 211.24 | Grade_3 | 67 | 8.60 | 232.35 | Grade_2 | 111 | 10.40 | 339.79 | Grade_1 | | | | |
| 24 | 13.20 | 547.39 | Grade_1 | 68 | 13.40 | 564.10 | Grade_1 | 112 | 12.40 | 483.05 | Grade_2 | | | | |
| 25 | 11.20 | 394.08 | Grade_2 | 69 | 10.70 | 359.68 | Grade_2 | 113 | 11.00 | 380.13 | Grade_2 | | | | |
| 26 | 8.10 | 206.12 | Grade_2 | 70 | 9.60 | 289.53 | Grade_1 | 114 | 10.50 | 346.36 | Grade_1 | | | | |
| 27 | 10.00 | 314.16 | Grade_2 | 71 | 12.80 | 514.72 | Grade_2 | 115 | 10.10 | 320.47 | Grade_2 | | | | |
| 28 | 14.10 | 624.58 | Grade_2 | 72 | 12.00 | 452.39 | Grade_2 | 116 | 14.10 | 624.58 | Grade_2 | | | | |
| 29 | 7.90 | 196.07 | Grade_2 | 73 | 7.80 | 191.13 | Grade_2 | 117 | 9.10 | 260.16 | Grade_1 | | | | |
| 30 | 8.40 | 221.67 | Grade_1 | 74 | 11.20 | 394.08 | Grade_2 | 118 | 6.50 | 132.73 | Grade_3 | | | | |
| 31 | 13.70 | 589.65 | Grade_2 | 75 | 6.30 | 124.69 | Grade_2 | 119 | 6.30 | 124.69 | Grade_3 | | | | |
| 32 | 10.10 | 320.47 | Grade_2 | 76 | 16.90 | 897.27 | Grade_2 | 120 | 9.60 | 289.53 | Grade_2 | | | | |
| 33 | 11.70 | 430.05 | Grade_2 | 77 | 11.10 | 387.08 | Grade_2 | 121 | 5.40 | 91.61 | Grade_2 | | | | |
| 34 | 14.00 | 615.75 | Grade_3 | 78 | 8.20 | 211.24 | Grade_2 | 122 | 5.40 | 91.61 | Grade_3 | | | | |
| 35 | 10.30 | 333.29 | Grade_2 | 79 | 12.10 | 459.96 | Grade_2 | 123 | 3.70 | 43.01 | Grade_1 | | | | |
| 36 | 8.30 | 216.42 | Grade_2 | 80 | 11.00 | 380.13 | Grade_2 | 124 | 6.40 | 128.68 | Grade_1 | | | | |
| 37 | 10.80 | 366.44 | Grade_3 | 81 | 8.00 | 201.06 | Grade_2 | 125 | 9.60 | 289.53 | Grade_2 | | | | |
| 38 | 7.60 | 181.46 | Grade_1 | 82 | 15.50 | 754.77 | Grade_2 | 126 | 8.10 | 206.12 | Grade_3 | | | | |
| 39 | 7.20 | 162.86 | Grade_2 | 83 | 10.50 | 346.36 | Grade_2 | 127 | 11.00 | 380.13 | Grade_2 | | | | |
| 40 | 15.70 | 774.37 | Grade_1 | 84 | 7.40 | 172.03 | Grade_2 | 128 | 9.80 | 301.72 | Grade_3 | | | | |
| 41 | 9.50 | 283.53 | Grade_2 | 85 | 8.70 | 237.79 | Grade_1 | 129 | 10.70 | 359.68 | Grade_2 | | | | |
| 42 | 14.60 | 669.66 | Grade_2 | 86 | 8.90 | 248.85 | Grade_3 | 130 | 10.00 | 314.16 | Grade_2 | | | | |
| 43 | 13.30 | 555.72 | Grade_2 | 87 | 7.70 | 186.27 | Grade_3 | 131 | 8.20 | 211.24 | Grade_2 | | | | |
| 44 | 8.60 | 232.35 | Grade_1 | 88 | 9.20 | 265.90 | Grade_1 | 132 | 5.30 | 88.25 | Grade_2 | | | | |
| Structural Cost (Best) | | | | 7.2535 | | | | Structural Cost (Mean) | | | | 12.163 | | | |
| Structural Cost (Worst) | | | | 27.9527 | | | | Standard Deviation | | | | 7.9349 | | | |

4.2. Transmission Tower 2

A transmission tower truss with 72 elements and 20 nodes is shown in Fig. 7 as the second example.

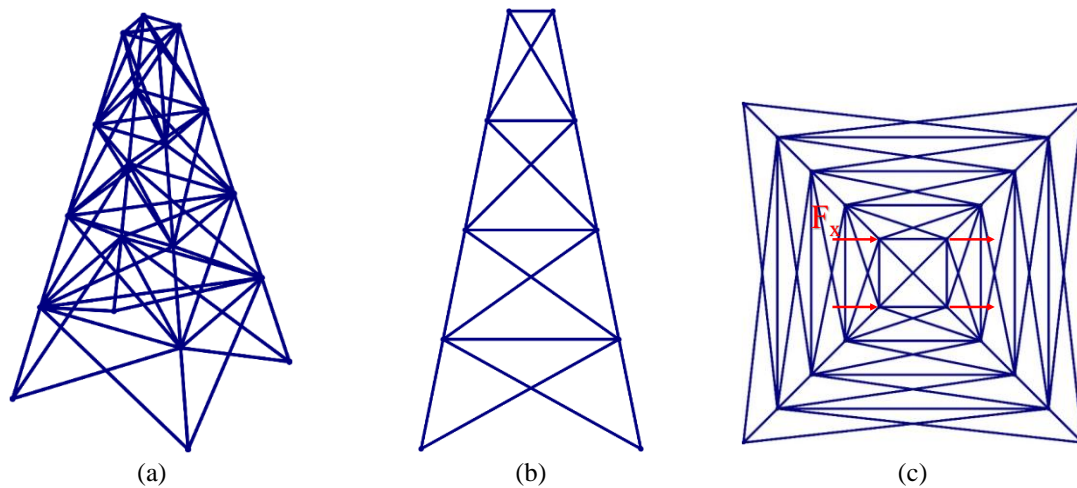


Figure 7: The initial configuration of the transmission tower 2: (a) 3D, (b) Front, and (c) Top views

As stated before, the optimization process was carried out ten times independently, with the cost of the trusses used in each run being recorded in Table 5. Similar to Example 1, the nodal coordinates and the elemental connectivity of the current example are available as Tables C3 and C4 in Complementary Tables.

Table 5: The optimal cost of the structure achieved by BHMO through each independent optimization procedure (Example 2)

| NFE (%) | Run 1 | Run 2 | Run 3 | Run 4 | Run 5 | Run 6 | Run 7 | Run 8 | Run 9 | Run 10 |
|--------------------------------|--------|--------|-----------------|--------|--------|-------------------------------|--------|---------|---------------|---------|
| 3 | 290.18 | 341.33 | 355.74 | 807.20 | 454.38 | 1206.74 | 465.93 | 2254.16 | 1934.03 | 2951.59 |
| 6 | 73.47 | 273.44 | 105.70 | 217.70 | 322.61 | 191.78 | 106.24 | 706.30 | 537.79 | 584.14 |
| 9 | 73.47 | 163.09 | 105.70 | 217.70 | 66.76 | 183.98 | 28.14 | 370.32 | 450.11 | 153.73 |
| 12 | 36.74 | 93.24 | 81.60 | 81.78 | 66.76 | 137.55 | 10.15 | 238.65 | 434.07 | 146.37 |
| 15 | 36.74 | 92.45 | 81.60 | 81.78 | 40.48 | 120.36 | 10.08 | 67.96 | 401.20 | 120.05 |
| 18 | 36.74 | 92.45 | 81.60 | 38.66 | 40.48 | 88.17 | 9.65 | 56.31 | 401.20 | 88.36 |
| 21 | 36.74 | 80.51 | 54.19 | 38.66 | 40.48 | 88.17 | 9.45 | 50.92 | 386.39 | 88.36 |
| 24 | 34.13 | 80.51 | 54.19 | 38.66 | 40.48 | 77.63 | 9.29 | 38.71 | 386.39 | 84.21 |
| 27 | 21.88 | 80.51 | 54.19 | 38.66 | 40.48 | 55.53 | 9.07 | 27.81 | 386.39 | 83.13 |
| 30 | 21.88 | 80.51 | 54.19 | 33.38 | 35.33 | 39.86 | 9.00 | 27.40 | 386.39 | 80.05 |
| 33 | 21.88 | 80.51 | 32.93 | 17.47 | 34.82 | 31.74 | 9.00 | 24.22 | 386.39 | 43.82 |
| 36 | 14.98 | 70.21 | 32.93 | 16.40 | 27.85 | 22.91 | 8.93 | 22.78 | 381.62 | 43.82 |
| 39 | 14.98 | 70.21 | 32.93 | 15.72 | 16.95 | 21.85 | 8.88 | 17.26 | 381.62 | 43.82 |
| 42 | 14.98 | 41.30 | 32.93 | 15.72 | 16.87 | 21.85 | 8.83 | 15.93 | 381.62 | 43.82 |
| 45 | 14.98 | 41.30 | 32.93 | 9.41 | 13.84 | 21.85 | 8.82 | 15.93 | 381.62 | 43.82 |
| 48 | 14.98 | 41.30 | 32.93 | 9.08 | 8.97 | 21.85 | 8.81 | 15.88 | 381.62 | 43.82 |
| 51 | 14.98 | 41.30 | 32.93 | 8.88 | 8.78 | 21.85 | 8.81 | 15.88 | 381.62 | 43.82 |
| 54 | 14.98 | 37.98 | 17.96 | 8.88 | 8.69 | 21.80 | 8.81 | 15.85 | 345.20 | 43.82 |
| 57 | 14.98 | 37.98 | 17.96 | 8.83 | 8.65 | 20.82 | 8.80 | 14.06 | 305.64 | 43.82 |
| 60 | 14.98 | 36.12 | 16.10 | 8.83 | 8.51 | 20.30 | 8.80 | 14.06 | 305.64 | 43.82 |
| 63 | 14.98 | 36.12 | 15.27 | 8.83 | 8.48 | 19.46 | 8.80 | 13.22 | 303.05 | 43.82 |
| 66 | 14.98 | 34.83 | 9.37 | 8.83 | 8.45 | 19.46 | 8.79 | 13.17 | 297.33 | 43.82 |
| 70 | 14.98 | 34.83 | 9.37 | 8.63 | 8.45 | 19.46 | 8.79 | 13.09 | 297.33 | 43.82 |
| 75 | 14.98 | 34.83 | 9.37 | 8.63 | 8.43 | 19.46 | 8.78 | 13.09 | 297.33 | 43.82 |
| 80 | 14.98 | 33.46 | 9.37 | 8.63 | 8.42 | 19.23 | 8.78 | 13.09 | 199.75 | 43.82 |
| 85 | 14.98 | 24.89 | 9.37 | 8.63 | 8.42 | 19.22 | 8.78 | 13.09 | 193.93 | 43.82 |
| 90 | 14.98 | 24.89 | 9.37 | 8.63 | 8.40 | 19.21 | 8.77 | 13.09 | 193.93 | 43.82 |
| 95 | 9.09 | 24.89 | 9.37 | 8.58 | 8.40 | 16.74 | 8.77 | 13.09 | 193.93 | 43.82 |
| 98 | 9.09 | 24.89 | 9.34 | 8.40 | 8.40 | 16.74 | 8.77 | 13.09 | 193.93 | 43.82 |
| 100 | 9.09 | 24.89 | 9.34 | 8.40 | 8.40 | 16.74 | 8.77 | 13.09 | 193.93 | 43.82 |
| Structural Cost (Best) | | | 8.397 | | | Structural Cost (Mean) | | | 33.648 | |
| Structural Cost (Worst) | | | 193.9303 | | | Standard Deviation | | | 57.413 | |

Following that, the history of the convergence of the most optimal procedure is displayed in Fig. (8), and Table 6 contains the solution of the current example. Finally, Figs. (9) and (10) confirmed that, with regard to elemental stress and nodal stress handling, respectively, the outcome of the procedure is without violation. Additionally, Fig. (11) demonstrates a schematic of a truss in the optimal decision.

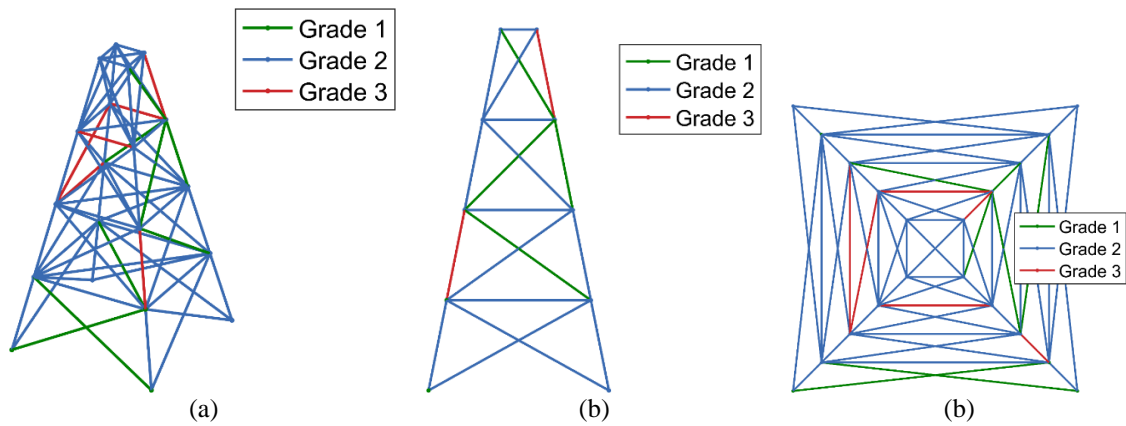


Figure 8: The optimized configuration of the transmission tower 2: (a) 3D, (b) Front, and (c) Top views

Table 6: The optimal decision variables of the best solution (Example 2)

| Element ID | Radius (cm) | Area (cm ²) | Material | Element ID | Radius (cm) | Area (cm ²) | Material |
|------------|-------------|-------------------------|----------|------------|-------------|-------------------------|----------|
| 1 | 14.1 | 624.58004 | Grade_2 | 37 | 8.9 | 248.85 | Grade_2 |
| 2 | 11 | 380.13271 | Grade_2 | 38 | 9.7 | 295.59 | Grade_2 |
| 3 | 5.9 | 109.35884 | Grade_1 | 39 | 11.9 | 444.88 | Grade_2 |
| 4 | 6.4 | 128.67964 | Grade_2 | 40 | 7.1 | 158.37 | Grade_2 |
| 5 | 7 | 153.93804 | Grade_2 | 41 | 7.4 | 172.03 | Grade_2 |
| 6 | 9.4 | 277.59113 | Grade_2 | 42 | 14.8 | 688.13 | Grade_2 |
| 7 | 18.3 | 1052.088 | Grade_2 | 43 | 8.7 | 237.79 | Grade_2 |
| 8 | 12.1 | 459.96058 | Grade_2 | 44 | 11.1 | 387.08 | Grade_2 |
| 9 | 13.6 | 581.06898 | Grade_1 | 45 | 11 | 380.13 | Grade_2 |
| 10 | 12.2 | 467.59465 | Grade_2 | 46 | 11.2 | 394.08 | Grade_3 |
| 11 | 10 | 314.15927 | Grade_2 | 47 | 9.1 | 260.16 | Grade_1 |
| 12 | 9.3 | 271.71635 | Grade_2 | 48 | 13.7 | 589.65 | Grade_2 |
| 13 | 11.7 | 430.05262 | Grade_2 | 49 | 12.6 | 498.76 | Grade_2 |
| 14 | 6.6 | 136.84778 | Grade_2 | 50 | 11.1 | 387.08 | Grade_2 |
| 15 | 11.2 | 394.08138 | Grade_2 | 51 | 12.3 | 475.29 | Grade_2 |
| 16 | 11.9 | 444.88094 | Grade_2 | 52 | 7.4 | 172.03 | Grade_2 |
| 17 | 5.9 | 109.35884 | Grade_2 | 53 | 15.1 | 716.31 | Grade_2 |
| 18 | 12.1 | 459.96058 | Grade_2 | 54 | 8.6 | 232.35 | Grade_2 |
| 19 | 15.3 | 735.41542 | Grade_3 | 55 | 10.7 | 359.68 | Grade_3 |
| 20 | 9.5 | 283.52874 | Grade_2 | 56 | 7.7 | 186.27 | Grade_2 |
| 21 | 8.7 | 237.78715 | Grade_2 | 57 | 11.1 | 387.08 | Grade_3 |
| 22 | 11.6 | 422.73271 | Grade_2 | 58 | 9.5 | 283.53 | Grade_3 |
| 23 | 11.6 | 422.73271 | Grade_1 | 59 | 13 | 530.93 | Grade_2 |
| 24 | 9.3 | 271.71635 | Grade_2 | 60 | 8.7 | 237.79 | Grade_2 |
| 25 | 11.9 | 444.88094 | Grade_2 | 61 | 9.7 | 295.59 | Grade_2 |
| 26 | 10.5 | 346.36059 | Grade_3 | 62 | 9.1 | 260.16 | Grade_2 |
| 27 | 13.1 | 539.12872 | Grade_2 | 63 | 13.6 | 581.07 | Grade_2 |
| 28 | 4.8 | 72.382295 | Grade_2 | 64 | 9 | 254.47 | Grade_2 |
| 29 | 12.8 | 514.71854 | Grade_2 | 65 | 10.6 | 352.99 | Grade_1 |
| 30 | 11.1 | 387.07563 | Grade_1 | 66 | 12.2 | 467.59 | Grade_2 |
| 31 | 12.8 | 514.71854 | Grade_2 | 67 | 8.7 | 237.79 | Grade_2 |
| 32 | 11.4 | 408.28138 | Grade_1 | 68 | 8.7 | 237.79 | Grade_2 |
| 33 | 11 | 380.13271 | Grade_2 | 69 | 7.2 | 162.86 | Grade_2 |
| 34 | 17.7 | 984.22956 | Grade_1 | 70 | 6.3 | 124.69 | Grade_2 |
| 35 | 7.8 | 191.1345 | Grade_2 | 71 | 8.6 | 232.35 | Grade_2 |
| 36 | 5.8 | 105.68318 | Grade_2 | 72 | 11.7 | 430.05 | Grade_2 |

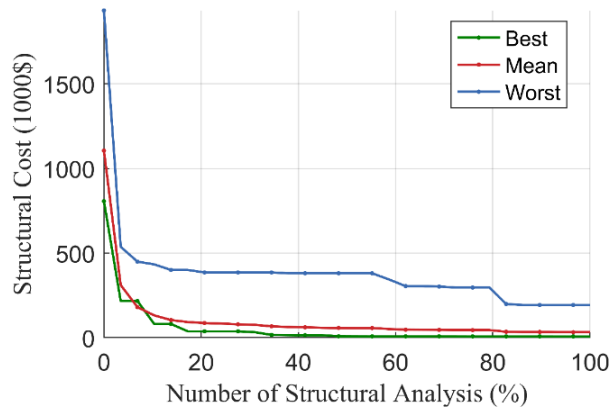


Figure 9: The optimization procedure of the transmission tower 2

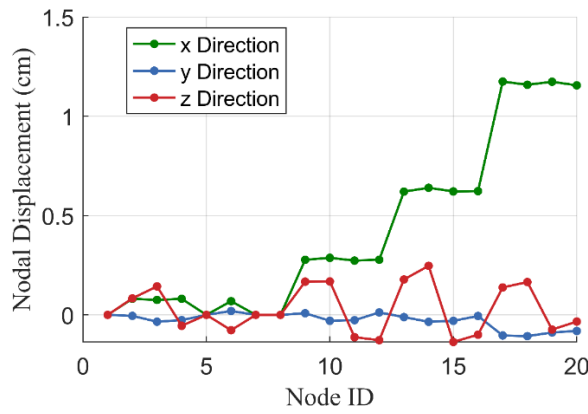


Figure 10: The nodal displacement of the transmission tower 2

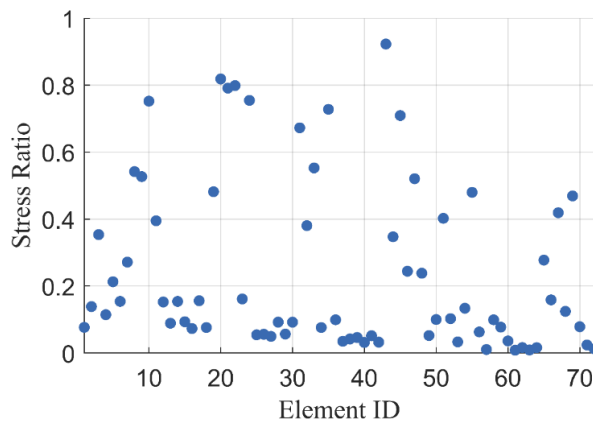


Figure 11: The element stress ratio of the transmission tower 2

4.3. Transmission Tower 3

The last numerical example is configured in Fig. (12).

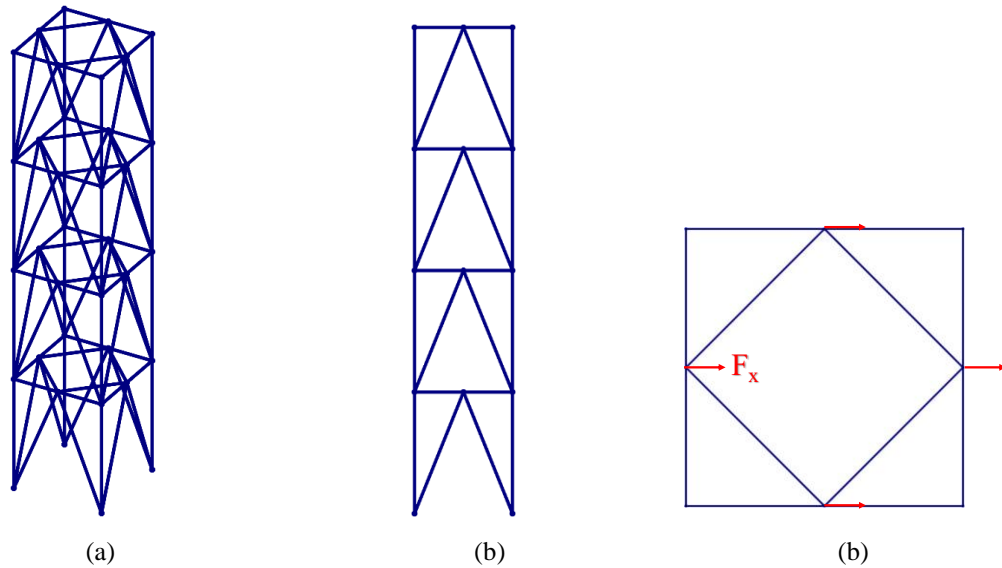


Figure 12: The initial configuration of the transmission tower 3: (a) 3D, (b) Front, and (c) Top views

Table 7 presents the cost results of 10 independent runs, including the best, worst, and average costs. Finally, the history of the best procedure’s solution among 10 independent runs demonstrated in Fig. (13) as well as the optimal decision for elements is tabulated in Table 8. The handling of constraints on the elemental stress and therefore, nodal displacement, along with the optimum schematic, which are respectively plotted in Figs. (14-16). The details of the nodal coordinate and element connectivity of Example 3 have been incorporated in Complementary Tables (Tables C5 and C6).

Table 7. The optimal cost of the structure achieved by BHMO through each independent optimization procedure (Example 3)

| NFE (%) | Run 1 | Run 2 | Run 3 | Run 4 | Run 5 | Run 6 | Run 7 | Run 8 | Run 9 | Run 10 |
|---------|-------|--------|--------|--------|---------|--------|---------|---------|--------|---------|
| 3 | 71.32 | 462.02 | 734.33 | 746.15 | 2048.32 | 922.12 | 1772.87 | 3089.86 | 891.86 | 3593.14 |
| 6 | 48.90 | 271.33 | 440.71 | 368.40 | 562.83 | 509.44 | 613.84 | 907.67 | 172.43 | 1204.36 |
| 9 | 48.90 | 271.33 | 284.45 | 147.47 | 452.63 | 372.85 | 613.84 | 451.75 | 133.13 | 633.15 |
| 12 | 48.90 | 161.49 | 284.45 | 110.97 | 320.28 | 364.47 | 546.01 | 167.87 | 130.43 | 625.59 |
| 15 | 48.90 | 161.49 | 284.45 | 97.68 | 268.13 | 364.47 | 384.60 | 162.76 | 88.00 | 536.42 |
| 18 | 48.90 | 161.49 | 194.80 | 35.14 | 181.56 | 313.79 | 355.84 | 96.77 | 71.87 | 494.95 |
| 21 | 48.90 | 161.49 | 194.80 | 30.82 | 144.91 | 313.79 | 99.64 | 78.93 | 65.30 | 482.86 |
| 24 | 48.90 | 161.49 | 186.33 | 15.55 | 125.98 | 280.02 | 81.26 | 58.39 | 58.63 | 460.27 |
| 27 | 48.90 | 161.49 | 186.33 | 14.50 | 125.98 | 264.08 | 55.05 | 49.75 | 54.81 | 460.27 |
| 30 | 48.90 | 161.49 | 175.52 | 14.50 | 125.98 | 189.75 | 44.92 | 35.28 | 45.16 | 460.27 |
| 33 | 48.35 | 150.40 | 175.52 | 14.50 | 125.98 | 112.59 | 35.51 | 14.67 | 16.05 | 446.86 |
| 36 | 48.35 | 150.40 | 175.52 | 7.77 | 125.98 | 112.59 | 33.99 | 14.55 | 16.05 | 446.86 |
| 39 | 48.35 | 150.40 | 154.52 | 7.77 | 125.98 | 95.64 | 33.99 | 14.45 | 16.05 | 445.69 |
| 42 | 37.92 | 150.40 | 103.76 | 7.68 | 125.98 | 88.53 | 33.37 | 11.20 | 13.27 | 445.69 |
| 45 | 37.92 | 150.40 | 103.07 | 7.54 | 123.38 | 88.45 | 32.50 | 11.20 | 13.27 | 424.49 |
| 48 | 29.64 | 150.40 | 103.07 | 7.54 | 123.38 | 88.45 | 32.31 | 11.20 | 13.27 | 414.39 |
| 51 | 29.64 | 145.21 | 103.07 | 7.54 | 123.38 | 88.45 | 32.20 | 11.19 | 12.77 | 396.67 |
| 54 | 29.64 | 136.89 | 103.07 | 7.54 | 123.38 | 88.45 | 29.21 | 11.17 | 12.77 | 396.67 |
| 57 | 27.97 | 115.99 | 103.07 | 7.48 | 123.38 | 88.45 | 27.59 | 11.17 | 12.77 | 396.67 |
| 60 | 27.97 | 115.99 | 103.07 | 7.48 | 121.73 | 88.45 | 27.45 | 11.17 | 12.77 | 396.67 |

| NFE (%) | Run 1 | Run 2 | Run 3 | Run 4 | Run 5 | Run 6 | Run 7 | Run 8 | Run 9 | Run 10 |
|--------------------------------|-------|--------|--------|---------------|--------|-------------------------------|-------|-------|-------|---------------|
| 63 | 27.97 | 110.06 | 103.07 | 7.48 | 121.73 | 88.45 | 27.45 | 11.17 | 12.77 | 396.67 |
| 66 | 27.97 | 110.06 | 95.96 | 7.48 | 121.73 | 88.45 | 27.45 | 11.17 | 12.77 | 396.67 |
| 70 | 27.97 | 73.89 | 73.81 | 7.46 | 121.73 | 88.45 | 27.45 | 11.17 | 12.77 | 396.67 |
| 75 | 27.97 | 73.89 | 73.81 | 7.45 | 121.73 | 88.45 | 27.45 | 11.17 | 12.77 | 396.67 |
| 80 | 27.97 | 73.89 | 73.58 | 7.45 | 121.73 | 88.45 | 27.45 | 11.17 | 12.77 | 396.67 |
| 85 | 23.94 | 73.89 | 72.42 | 7.45 | 121.73 | 88.45 | 27.45 | 11.17 | 12.77 | 396.67 |
| 90 | 23.94 | 73.89 | 72.42 | 7.45 | 121.73 | 88.45 | 27.45 | 11.17 | 12.77 | 396.67 |
| 95 | 22.16 | 73.89 | 72.42 | 7.45 | 121.73 | 88.45 | 27.45 | 11.17 | 12.77 | 396.67 |
| 98 | 22.16 | 49.81 | 72.42 | 7.45 | 121.73 | 88.45 | 27.45 | 11.17 | 12.77 | 396.67 |
| 100 | 9.03 | 46.59 | 72.42 | 7.45 | 121.73 | 88.45 | 27.45 | 11.17 | 12.77 | 396.67 |
| Structural Cost (Best) | | | | 7.4483 | | Structural Cost (Mean) | | | | 79.374 |
| Structural Cost (Worst) | | | | 396.67 | | Standard Deviation | | | | 118.13 |

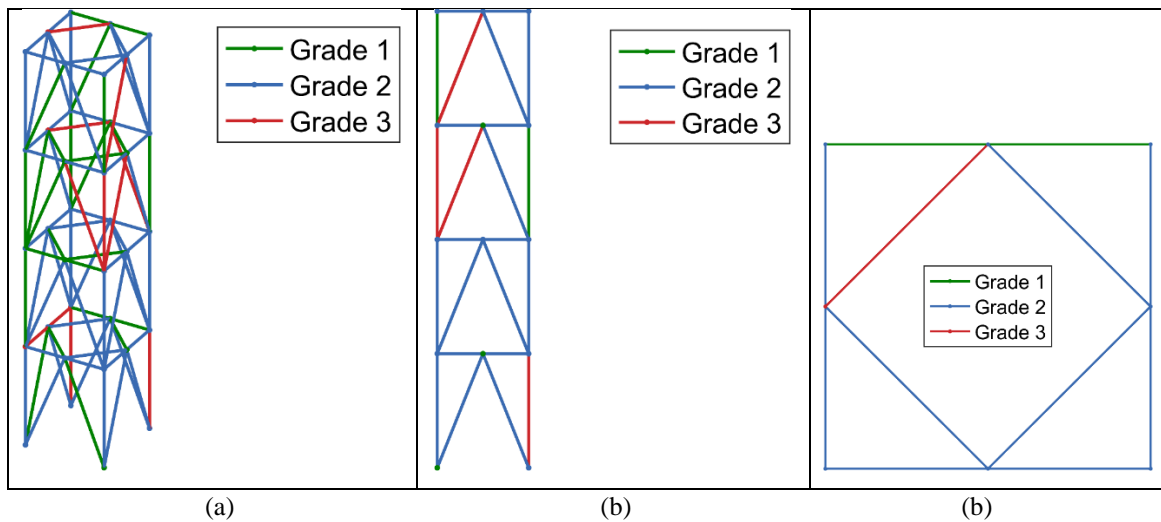


Figure 13. The optimized configuration of the transmission tower 3: (a) 3D, (b) Front, and (c) Top views

Table 8. The optimal decision variables of the best solution (Example 3)

| Element ID | Radius (cm) | Area (cm ²) | Material | Element ID | Radius (cm) | Area (cm ²) | Material |
|------------|-------------|-------------------------|----------|------------|-------------|-------------------------|----------|
| 1 | 10.90 | 373.25 | Grade_2 | 41 | 14.80 | 688.13 | Grade_2 |
| 2 | 4.20 | 55.42 | Grade_1 | 42 | 14.50 | 660.52 | Grade_1 |
| 3 | 10.50 | 346.36 | Grade_2 | 43 | 9.30 | 271.72 | Grade_1 |
| 4 | 7.00 | 153.94 | Grade_3 | 44 | 17.50 | 962.11 | Grade_3 |
| 5 | 12.10 | 459.96 | Grade_2 | 45 | 12.40 | 483.05 | Grade_2 |
| 6 | 11.60 | 422.73 | Grade_2 | 46 | 12.60 | 498.76 | Grade_2 |
| 7 | 15.30 | 735.42 | Grade_2 | 47 | 9.50 | 283.53 | Grade_2 |
| 8 | 11.50 | 415.48 | Grade_2 | 48 | 15.40 | 745.06 | Grade_2 |
| 9 | 13.90 | 606.99 | Grade_1 | 49 | 13.90 | 606.99 | Grade_2 |
| 10 | 13.10 | 539.13 | Grade_3 | 50 | 6.00 | 113.10 | Grade_1 |
| 11 | 9.70 | 295.59 | Grade_2 | 51 | 5.10 | 81.71 | Grade_3 |
| 12 | 11.80 | 437.44 | Grade_2 | 52 | 12.40 | 483.05 | Grade_2 |
| 13 | 16.40 | 844.96 | Grade_1 | 53 | 11.40 | 408.28 | Grade_1 |
| 14 | 9.60 | 289.53 | Grade_2 | 54 | 9.30 | 271.72 | Grade_2 |
| 15 | 8.50 | 226.98 | Grade_2 | 55 | 12.00 | 452.39 | Grade_2 |
| 16 | 12.10 | 459.96 | Grade_2 | 56 | 9.80 | 301.72 | Grade_2 |
| 17 | 7.20 | 162.86 | Grade_2 | 57 | 8.10 | 206.12 | Grade_2 |
| 18 | 11.10 | 387.08 | Grade_2 | 58 | 6.60 | 136.85 | Grade_2 |
| 19 | 13.60 | 581.07 | Grade_2 | 59 | 8.80 | 243.28 | Grade_2 |
| 20 | 8.40 | 221.67 | Grade_2 | 60 | 10.00 | 314.16 | Grade_2 |

| Element ID | Radius (cm) | Area (cm ²) | Material | Element ID | Radius (cm) | Area (cm ²) | Material |
|------------|-------------|-------------------------|----------|------------|-------------|-------------------------|----------|
| 21 | 12.00 | 452.39 | Grade_2 | 61 | 10.90 | 373.25 | Grade_2 |
| 22 | 14.20 | 633.47 | Grade_2 | 62 | 8.90 | 248.85 | Grade_1 |
| 23 | 15.00 | 706.86 | Grade_2 | 63 | 5.60 | 98.52 | Grade_2 |
| 24 | 11.90 | 444.88 | Grade_2 | 64 | 12.80 | 514.72 | Grade_2 |
| 25 | 16.50 | 855.30 | Grade_1 | 65 | 12.10 | 459.96 | Grade_1 |
| 26 | 5.50 | 95.03 | Grade_1 | 66 | 9.40 | 277.59 | Grade_2 |
| 27 | 12.10 | 459.96 | Grade_1 | 67 | 14.40 | 651.44 | Grade_2 |
| 28 | 9.70 | 295.59 | Grade_1 | 68 | 11.60 | 422.73 | Grade_1 |
| 29 | 10.10 | 320.47 | Grade_2 | 69 | 4.50 | 63.62 | Grade_1 |
| 30 | 14.90 | 697.46 | Grade_1 | 70 | 6.20 | 120.76 | Grade_2 |
| 31 | 12.10 | 459.96 | Grade_3 | 71 | 7.10 | 158.37 | Grade_1 |
| 32 | 6.80 | 145.27 | Grade_3 | 72 | 15.60 | 764.54 | Grade_2 |
| 33 | 15.60 | 764.54 | Grade_3 | 73 | 11.70 | 430.05 | Grade_1 |
| 34 | 14.50 | 660.52 | Grade_1 | 74 | 3.70 | 43.01 | Grade_3 |
| 35 | 10.00 | 314.16 | Grade_2 | 75 | 13.10 | 539.13 | Grade_1 |
| 36 | 10.70 | 359.68 | Grade_3 | 76 | 12.90 | 522.79 | Grade_1 |
| 37 | 12.00 | 452.39 | Grade_2 | 77 | 11.40 | 408.28 | Grade_2 |
| 38 | 18.40 | 1063.62 | Grade_2 | 78 | 9.00 | 254.47 | Grade_3 |
| 39 | 14.20 | 633.47 | Grade_1 | 79 | 9.30 | 271.72 | Grade_2 |
| 40 | 7.90 | 196.07 | Grade_2 | 80 | 8.90 | 248.85 | Grade_2 |

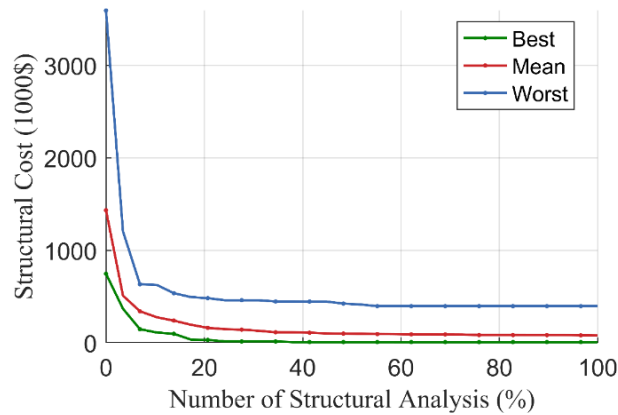


Figure 14: The optimization procedure of the transmission tower 3

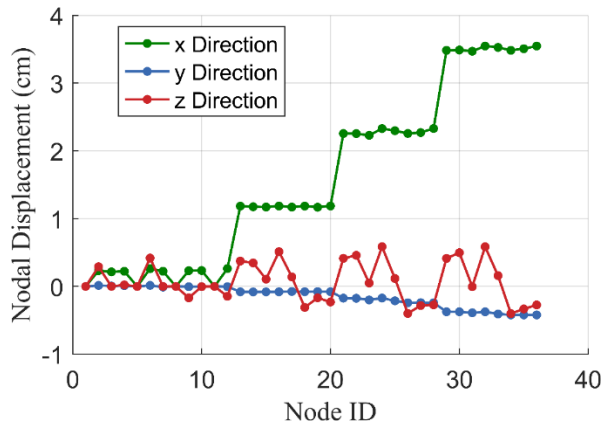


Figure 15: The nodal displacement of the transmission tower 3

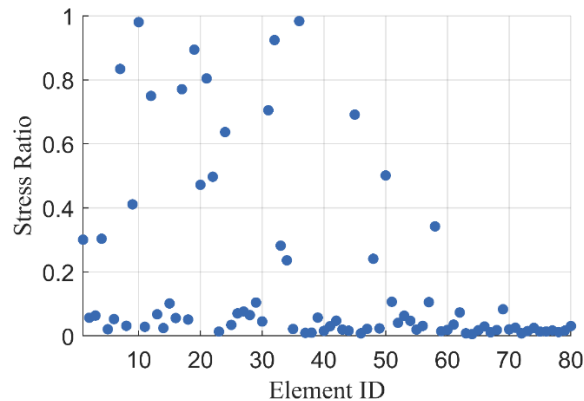


Figure 16: The element stress ratio of the transmission tower 3

5. CONCLUSION

In the present research, a multi-material size optimization of transmission tower structures is carried out using the BHMO metaheuristic algorithm. Thus, by taking into account a list of discrete size variables using a trio of kinds of steel material, three real-size instances of transmission truss towers were designed and then optimized. In the first example, characterized by 72 nodes and 132 bar elements and classified as a real-size transmission tower, the proposed algorithm was employed for optimization, resulting in a notable 46 percent reduction in the total structural cost. In the second example, featuring 72 bar elements and 20 nodes, optimization yielded an impressive 64 percent reduction in total structural cost when compared to the initial design. Lastly, the third example, comprising 36 nodes and 80 bar elements and classified as a real-size transmission tower, achieved a substantial 55 percent optimization in total structural cost relative to conventional design specifications. Results demonstrate the effectiveness of the BHMO in addressing this problem. One can design a transmission tower using less costly steel since it not only has a reduced material density but also results in an optimal design that is lighter.

Future research can examine using the BHMO as a reliable optimizer in machine learning algorithms as well as other sorts of optimization problems like frame optimization or reverse optimization problems like damage detection of structures. Additionally, different metaheuristics may be used to optimize the tree in newly designed transformation tower trusses.

REFERENCES

1. Khodzhaiev M., Reuter U. Structural optimization of transmission towers using a novel Genetic Algorithm approach with a variable length genome. *Eng Struct.* 2021; **240**:112306.
2. Kaveh A. *Advances in Metaheuristic Algorithms for Optimal Design of Structures*. Cham: Springer International Publishing; 3rd edition, 2021.

3. Tort C., Şahin S., Hasançebi O. Optimum design of steel lattice transmission line towers using simulated annealing and PLS-TOWER. *Comput Struct.* 2017; **179**:75–94.
4. Kaveh A., Sheikholeslami R., Talatahari S., Keshvari-Ilkhichi M. Chaotic swarming of particles: A new method for size optimization of truss structures. *Adv Eng Softw.* 2014; **67**:136–47.
5. Adeli H., Cheng N. Integrated Genetic Algorithm for Optimization of Space Structures. *J Aerosp Eng.* 1993. **6**:315–28.
6. Kaveh A., Seddighian M. R., Ghanadpour E. Black Hole Mechanics Optimization: a novel meta-heuristic algorithm. *Asian J Civ Eng.* 2020; **21**:1129–49.
7. Hasançebi O., Kazemzadeh Azad S. Discrete sizing of steel frames using adaptive dimensional search algorithm. *Period Polytech Civ Eng.* 2019.
8. Pouriyanezhad E., Rahami H., Mirhosseini S. M. Truss optimization using eigenvectors of the covariance matrix. *Eng Comput.* 2021; **37**:2207–24.
9. Kaveh A., Seddighian M. R. Simultaneously multi-material layout and connectivity optimization of truss structures via an Enriched Firefly Algorithm. *Structures.* 2020; **27**:2217–31.
10. Awad R. Sizing optimization of truss structures using the political optimizer (PO) algorithm. *Structures.* 2021; **33**:4871–94.
11. Bodalal R., Shuaeib F. Marine Predators Algorithm for Sizing Optimization of Truss Structures with Continuous Variables. *Computation.* 2023; **11**:91.
12. Kaveh A., Shabani Rad A. Metaheuristic-based optimal design of truss structures using algebraic force method. *Structures.* 2023; **50**:1951–64.
13. Moez H., Kaveh A., Taghizadieh N. Natural Forest Regeneration Algorithm for Optimum Design of Truss Structures with Continuous and Discrete Variables. *Period Polytech Civ Eng.* 2016; **60**:257–67.
14. Kaveh A., Kabir M. Z., Bohlool M. Optimum design of three-dimensional steel frames with prismatic and non-prismatic elements. *Eng Comput.* 2020; **36**:1011–27.
15. Kaveh A., Kabir M. Z., Bohlool M. Optimal design of multi-span pitched roof frames with tapered members. *Period Polytech Civ Eng.* 2018; **63**(1): 77–86.
16. Kaveh A., Seddighian M. R. Optimization of slope critical surfaces considering seepage and seismic effects using finite element method and five meta-heuristic algorithms. *Period Polytech Civ Eng.* 2021; **65**(2): 425–36.
17. Kaveh A., Seddighian M. R. A new nodal stress recovery technique in finite element method using colliding bodies optimization algorithm. *Period Polytech Civ Eng.* 2019; **63**(4): 1159–70.
18. Sheppard D. J., Palmer A. C. Optimal design of transmission towers by dynamic programming. *Comput Struct.* 1972; **2**:455–68.
19. Rao G. V. Optimum designs for transmission line towers. *Comput Struct.* 1995; **57**:81–92.
20. Kaveh A., Gholipour Y., Rahami H. Optimal design of transmission towers using genetic algorithm and neural networks. *Int J Space Struct.* 2008; **23**:1–19.
21. Mathakari S., Gardoni P., Agarwal P., Raich A., Haukaas T. Reliability-based optimal design of electrical transmission towers using multi-objective genetic algorithms. *Comput Aided Civ Infrastruct Eng.* 2007; **22**:282–92.

22. Rajeev S., Krishnamoorthy C. S. Discrete optimization of structures using genetic algorithms. *J Struct Eng.* 1992; **118**:1233–50.
23. Couceiro I., París J., Martínez S., Colominas I., Navarrina F., Casteleiro M. Structural optimization of lattice steel transmission towers. *Eng Struct.* 2016; **117**:274–86.
24. Shea K., Smith I. F. C. Improving Full-Scale Transmission Tower Design through Topology and Shape Optimization. *J Struct Eng.* 2006; **132**:781–90.
25. Jafari M., Salajegheh E., Salajegheh J. Optimal design of truss structures using a hybrid method based on particle swarm optimizer and cultural algorithm. *Structures.* 2021; **32**:391–405.
26. Zhengtong H., Zhengqi G., Xiaokui M., Wanglin C. Multimaterial layout optimization of truss structures via an improved particle swarm optimization algorithm. *Comput Struct.* 2019; **222**:10–24.
27. Souza R. R. de, Fadel Miguel L. F., Lopez R. H., Miguel L. F. F., Torii A. J. A procedure for the size, shape, and topology optimization of transmission line tower structures. *Eng Struct.* 2016; **111**:162–84.
28. Lu S., Ma H., Xin L., Zuo W. Lightweight design of bus frames from multi-material topology optimization to cross-sectional size optimization. *Eng Optim.* 2019; **51**:961–77.
29. Zhang X. S., Paulino G. H., Ramos A. S. Multi-material topology optimization with multiple volume constraints: a general approach applied to ground structures with material nonlinearity. *Struct Multidiscip Optim.* 2018; **57**:161–82.
30. Zheng Y., Da D., Li H., Xiao M., Gao L. Robust topology optimization for multi-material structures under interval uncertainty. *Appl Math Model.* 2020; **78**:627–47.
31. Stanković T., Mueller J., Egan P., Shea K. A generalized optimality criteria method for optimization of additively manufactured multimaterial lattice structures. *J Mech Des.* 2015; **137**.
32. Goldberg D. E. Design of Competent Genetic Algorithms. 2002; pp. 187–216.
33. Kennedy J., Eberhart R. Particle swarm optimization. *Proc ICNN Int Conf Neural Netw.* IEEE; pp. 1942–8.
34. Dorigo M., Birattari M., Stutzle T. Ant colony optimization. *IEEE Comput Intell Mag.* 2006; **1**:28–39.
35. Hansen N. The CMA Evolution Strategy: A Comparing Review. *Toward New Evol Comput.* Berlin, Heidelberg: Springer Berlin Heidelberg; pp. 75–102.
36. Atashpaz-Gargari E., Lucas C. Imperialist competitive algorithm: An algorithm for optimization inspired by imperialistic competition. *Proc IEEE Congr Evol Comput.* 2007; pp. 4661–7.
37. Rao R. V., Savsani V. J., Vakharia D. P. Teaching–learning-based optimization: A novel method for constrained mechanical design optimization problems. *Comput Aided Des.* 2011; **43**:303–15.
38. Kirkpatrick S., Gelatt C. D., Vecchi M. P. Optimization by Simulated Annealing. *Science.* 1983; **220**:671–80.
39. Glover F. Tabu Search—Part I. *ORSA J Comput.* 1989; **1**:190–206.
40. Zong Woo Geem, Joong Hoon Kim, Loganathan G. V. A New Heuristic Optimization Algorithm: Harmony Search. *Simul.* 2001; **76**:60–8.